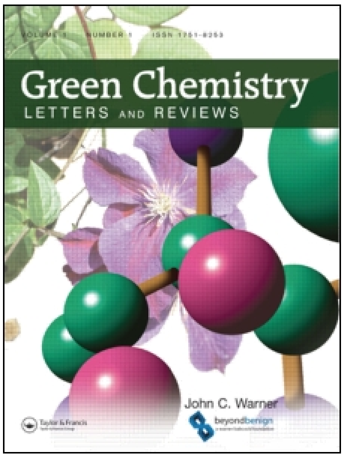

Green Chemistry Letters and Reviews
Publication details, including instructions for authors and subscription information:
http://www.informaworld.com/smpp/title~content=t748292817

The use of nano supported nickel catalyst in reduction of *p*-nitrophenol using hydrazine as hydrogen donor

Islam Hamdy Abd El Maksod[a,b]; Tamer S. Saleh[c]
[a] Physical Chemistry Department, National Research Centre, Cairo, Egypt [b] Chemistry Department, Faculty of Science, King Abdul Aziz University, Jeddah, Saudi Arabia [c] Green Chemistry Department, National Research Centre, Cairo, Egypt

To cite this Article Abd El Maksod, Islam Hamdy and Saleh, Tamer S.(2010) 'The use of nano supported nickel catalyst in reduction of *p*-nitrophenol using hydrazine as hydrogen donor', Green Chemistry Letters and Reviews, 3: 2, 127 — 134
To link to this Article: DOI: 10.1080/17518251003596143
URL: http://dx.doi.org/10.1080/17518251003596143

Green Chemistry Letters and Reviews
Vol. 3, No. 2, June 2010, 127–134

Taylor & Francis
Taylor & Francis Group

RESEARCH LETTER

The use of nano supported nickel catalyst in reduction of *p*-nitrophenol using hydrazine as hydrogen donor

Islam Hamdy Abd El Maksod[a,b] and Tamer S. Saleh[c]*

[a]*Physical Chemistry Department, National Research Centre, Cairo 12622, Egypt;* [b]*Chemistry Department, Faculty of Science, King Abdul Aziz University, Jeddah 21533, Saudi Arabia;* [c]*Green Chemistry Department, National Research Centre, Cairo 12622, Egypt*

(Received 19 April 2009; final version received 23 November 2009)

p-Aminophenol was prepared by hydrogenation of *p*-nitro phenol over nano-sized nickel catalysts supported on two different supports, SiO_2 and Al_2O_3. Hydrazine hydrate was used as hydrogen source in this reaction. Several loadings of nano-sized Ni were used, thus 20, 5, and 2.5 wt% were prepared. X-ray diffraction (XRD) and electron spin resonance (ESR) were employed to investigate the prepared catalysts. The Ni/Al_2O_3 was found to be more effective and give high durability. The catalytic activity of the reaction was found to be influenced by both the crystallinity of the nickel and the strain among nano-sized nickel particles. The prepared catalysts showed higher catalytic activity, especially at lower loading. During the reaction, a detectable change of the color was observed from yellow to green and finally to colorless, which enable us to suppose a mechanism of this reaction.

Keywords: nano nickel; hydrogenation; *p*-nitrophenol; *p*-aminophenol; catalytic activity; XRD; ESR

Introduction

Catalysis is considered to be highly valuable in science. This is partly because using the appropriate catalyst will reduce energy and thus reduce the impact on the environment. In addition, catalysis is listed as one of the principles of green chemistry. The most important challenge in catalysis is to synthesize a catalyst with 100% yield and 100% selectivity. With respect to the environment, the catalyst that reduces waste and is economical will be the better catalyst (*1,2*).

p-Aminophenol (PAP) is considered to be one of the most important intermediates in the manufacturing of many analgesic and antipyretic drugs, such as paracetamol, acetanilide, and Phentacin (*3–9*). It can be also utilized as a developer in photography with trade names of activol and azol and also in chemical dye industries (*10*).

There are many methods used in the preparation of PAP from *p*-nitrophenol (PNP) such as metal/acid reduction (*11*), catalytic hydrogenation (*12*), electrolytic reduction (*13*), homogeneous catalytic transfer hydrogenation (*14*), and heterogeneous catalytic transfer hydrogenation. Although all of these methods are still used today, each method has its shortcoming. For instance, the metal/acid system is not selective and requires strong acidic medium. The catalytic hydrogenation uses hydrogen gas with drastic conditions at high pressure. The electrolytic reduction needs acidic or alkaline catholite, and the desired product yield is very low. The homogeneous catalytic hydrogenation uses expensive catalysts in the form of complexes. Although the heterogeneous catalytic hydrogenation with supported metals (palladium, platinum, or ruthenium) is very effective, the complexes need special attention while dealing with them, because of their flammable nature in the presence of air.

Among all previously mentioned methods, direct catalytic hydrogenation of PNP to PAP becomes the most important one, because it could be an efficient and greener route for synthesis (*9*). Raney nickel (*15*), nano-sized nickel (*16*), and several noble metal catalysts such as Pd/C[9] have been used as catalysts for this reaction. Due to their cost-effectiveness and their higher catalytic activity, supported nickel catalysts are widely used in such reactions (*17–23*). Although the supported and unsupported nickel catalysts have been used for a long time in hydrogenation reactions, only a few recently published manuscripts deal with hydrogenation of PNP with nano nickel metal catalysts (*24–27*).

Most of this recent research used nano supported or unsupported nickel metal catalyst with high pressure of molecular hydrogen as a hydrogen source. Although nano nickel catalyst showed high catalytic activity, it requires high relative temperature and

---

*Corresponding author. Email: tamsaid@yahoo.com

ISSN 1751-8253 print/ISSN 1751-7192 online

DOI: 10.1080/17518251003596143
http://www.informaworld.com

pressure, which is not economically viable. The use of alternative hydrogen sources for hydrogenation of PNP to PAP has been reported very little in the literature. For example, hydrazinum monoformate was used with Raney nickel as an alternative hydrogen source for the hydrogenation of aromatic nitro compounds (*25*). However, the use of hydrazine monoformate has several disadvantages such as the possibility of interaction of nickel with a formate anion to form nickel format.

In this manuscript, we report herein on the utility of hydrazine hydrate as an alternative source of hydrogen with supported nano nickel catalysts as a system for reduction of aromatic nitro compounds using PNP as an example. Only H_2 and N_2 are the products of the catalytic decomposition of hydrazine hydrate used over nano-sized nickel catalyst in this reduction system. We used SiO_2 and Al_2O_3 as supports for the nano nickel particles comparing them to unsupported commercial Raney nickel catalyst. XRD and ESR techniques were employed to characterize the prepared nano-sized nickel catalysts.

Results

XRD studies

XRD analysis was applied to follow up the change in the crystallinity of Ni metal phase before and after using the catalysts samples in the reaction. Thus, the Ni metal phase (Figure 1(a)) in 20 wt% Ni/SiO_2 catalyst sample exhibits an observable degree of crystallinity. Moreover, after using the catalyst for five successive times with a ratio of 1:5 wt:wt Ni:PNP nearly no crystalline Ni could be observed from XRD diffractograms (Figure 1(b)).

In contrast to the supported SiO_2 catalyst, the degree of the crystallinity of Ni on the Al_2O_3 support remains nearly unchanged after using the catalyst for five times under the same conditions (Figure 2). This may be explained by the possibility of easier transformation of nickel from crystalline into amorphous phase on SiO_2 than that on Al_2O_3 support. Moreover, this may be related to the difference in metal support interaction between SiO_2 and Al_2O_3.

Furthermore, the XRD diffractograms of 5 wt% Ni/SiO_2 catalyst before and after using two times with ratio 1:5 wt:wt Ni:PNP (Figure 3), showed a sharp decrease in the degree of crystallinity of Ni metal after only two times of use.

In contrast, the XRD diffractograms of 5 wt% Ni/Al_2O_3 catalyst before and after using five times with ratio 1:5 wt:wt Ni:PNP (Figure 4), exhibit only a very small change in the degree of crystallinity of Ni metal.

Moreover, the XRD diffractograms of 2.5 wt% Ni/SiO_2 and Ni/Al_2O_3 catalysts showed no crystalline Ni metal at all which attributed to the very small amount of Ni loaded being beyond the detection limit of the XRD technique. The crystallite size of Ni for all samples under investigation was determined according to the Scherrer equation (*28*):

$$d = 0.941\lambda / B\cos\theta_B,$$

where λ is the wavelength, B is the full width at half maximum (FWHM) of the Bragg's peak corrected using the corresponding peak in micro-sized powder, and θ_B is the Bragg's angle.

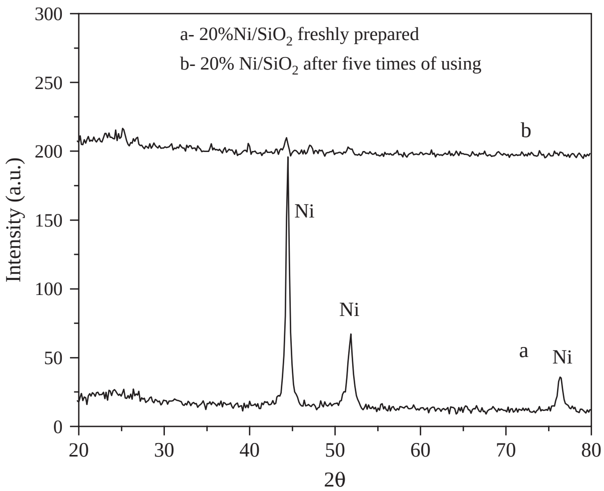

Figure 1. XRD diffractograms of 20 wt% Ni/SiO_2 catalyst (a) freshly prepared and (b) after fifth time of using.

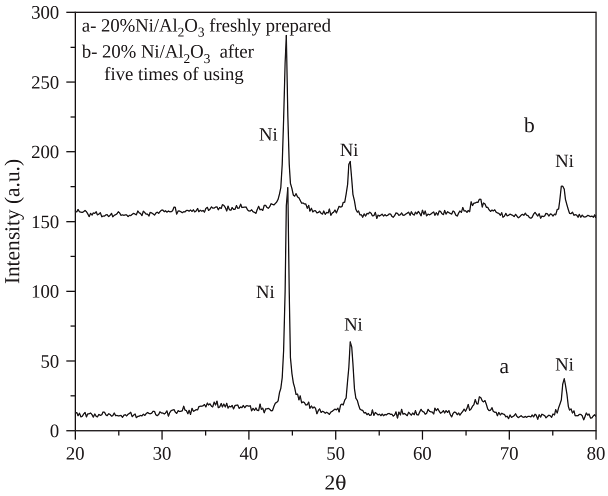

Figure 2. XRD diffractograms of 20 wt% Ni/Al_2O_3 catalyst (a) freshly prepared and (b) after fifth time of use.

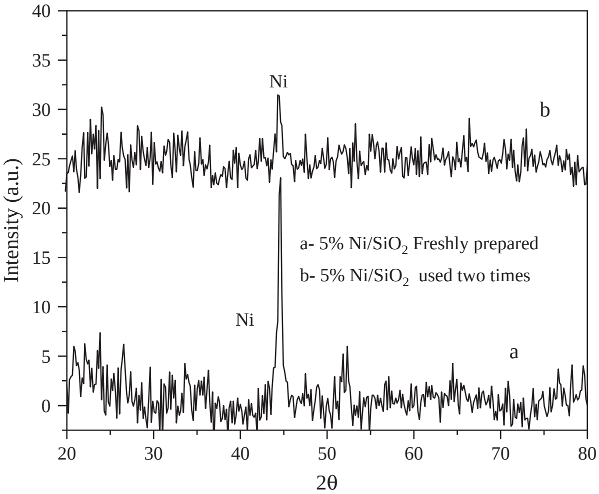

Figure 3. XRD diffractograms of 5 wt% Ni/SiO_2 catalyst (a) freshly prepared and (b) after second time of use.

ESR spectra

The ESR technique is employed in this research to investigate the nickel metal on different catalyst samples before and after use in the hydrogenation reaction. The ESR signals were found to be suffering from severe anisotropy (Figures 5–11), especially at higher loading concentrations. In addition, lower magnetic field signals are observed and found to overlap the other signals over the whole range of the magnetic field. This may be explained if we assume a spin–spin interaction to exist. To explain this assumption, it may be better to take a look at the electronic configuration of the nickel metal. Thus, $Ni^{(0)}$ contains two electrons in the 3d orbital; however, these electrons seem to be degenerate and can not result in such severe interactions appearing in the ESR spectra. The only remaining possibility to explain this phenomenon is that there is a spin–spin interaction between nano nickel particles or, in other words, strain between nano nickel particles (*28–30*).

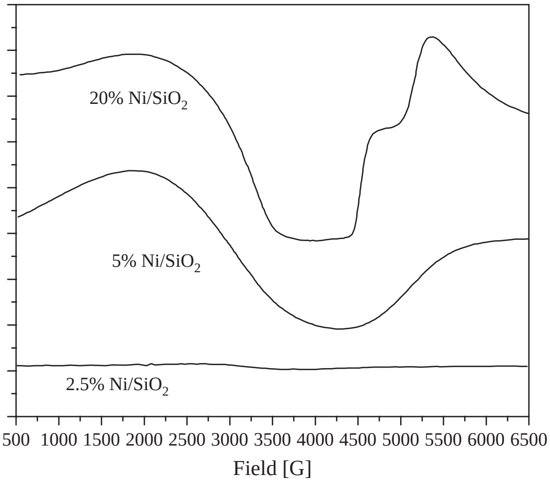

Figure 5. ESR spectra of 2.5, 5, and 20 wt% Ni/SiO_2 catalyst.

To prove this assumption, we make a successive solid–solid dilution of each sample with its bare support until all anisotropy of the ESR signal disappears (i.e. only one isotropic signal centered at $g = 2.2$ related to nickel metal appeared, e.g. Figure 11). From this signal, the particle size of nickel can be estimated. Thus, in 1970 Kawabata (*31*) demonstrated his famous relation hypothesizing that the broadening of ESR signal of nano metal particles is affected by the quantum size effect and can be correlated to the size of the nano metal particle.

Accordingly, direct relationship between the line width ΔH_{pp} (or peak-to-peak width) of the signal of

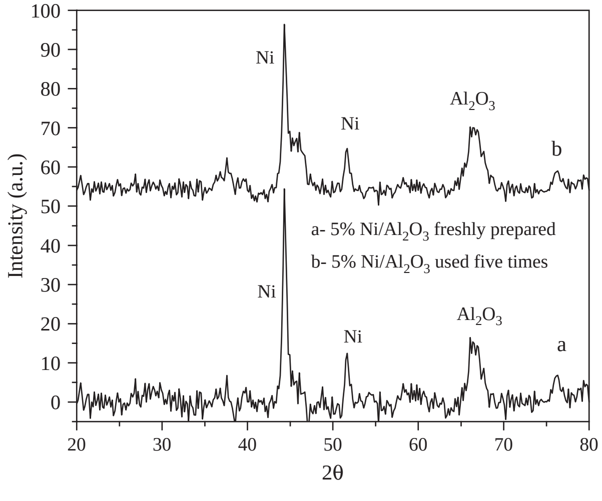

Figure 4. XRD diffractograms of 5 wt% Ni/Al_2O_3 catalyst (a) freshly prepared and (b) after fifth time of use.

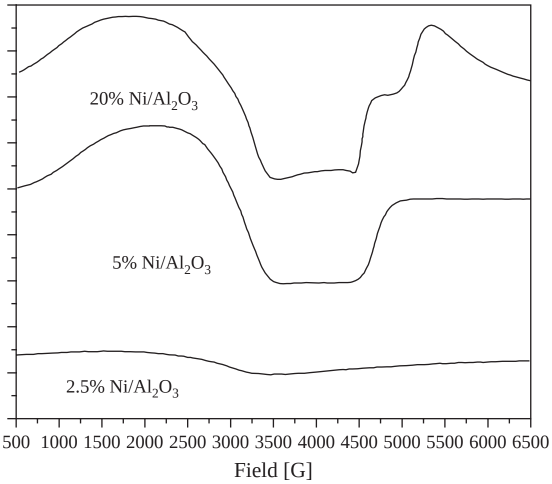

Figure 6. ESR spectra of 2.5, 5, and 20 wt% Ni/Al_2O_3 catalyst.

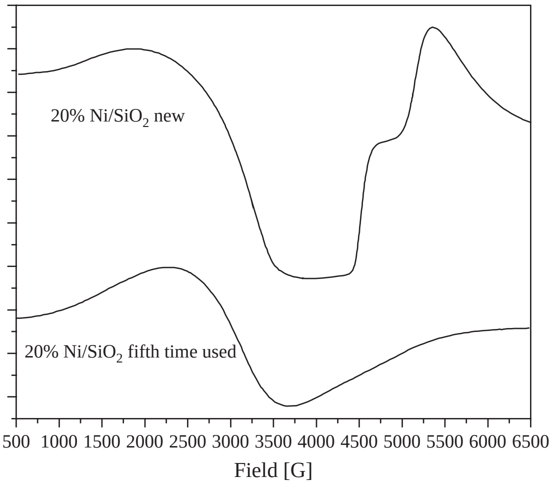

Figure 7. ESR spectra of 20 wt% Ni/SiO$_2$ catalyst, freshly prepared and after fifth time of using at 1:5 wt:wt of Ni:PNP.

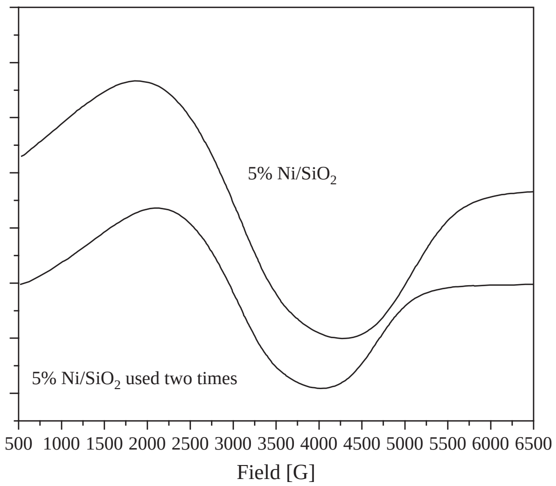

Figure 9. ESR spectra of 5 wt% Ni/SiO$_2$ catalyst, freshly prepared and after fifth time of using at 1:5 wt:wt of Ni:PNP.

nano particle in ESR spectra and its particle size is given in the following relation:

$$d = a(\Delta H_{pp})^{0.5}, \quad (1)$$

where d is the particle size in nm, ΔH_{pp} is the line width of ESR signal in mT, and a is the proportionality constant.

The proportionality constant "*a*" for nickel was previously determined as 1.2 (*32*). The particle size of investigated samples was calculated in Table 1.

In addition to the previous phenomenon, much useful information can be extracted by deeply analyzing the ESR spectra of samples under investigations. Thus from Figures 5 and 6, it can be observed that as the amount of loading of Ni increases, the amount of anisotropy of the ESR signal increases. Also 2.5 wt% Ni loading samples for both SiO$_2$ and Al$_2$O$_3$ showed nearly no signal which can be explained that at this concentration nearly no reduction of Ni can take place at these mild conditions of reduction.

Moreover, it can observed that the amount of anisotropy is proportional to the amount of crystalline Ni metal. Thus, in Figure 7 the fifth use of 20 wt% Ni/SiO$_2$ catalyst showed nearly no anisotropy accompanied with a sharp decrease in crystallinity of Ni as confirmed by XRD diffractograms (Figure 1). Moreover, anisotropy was still observed in the fifth use of 20 wt% Ni/Al$_2$O$_3$ catalyst where XRD diffractograms showed that it still has a crystalline Ni metal (Figure 2).

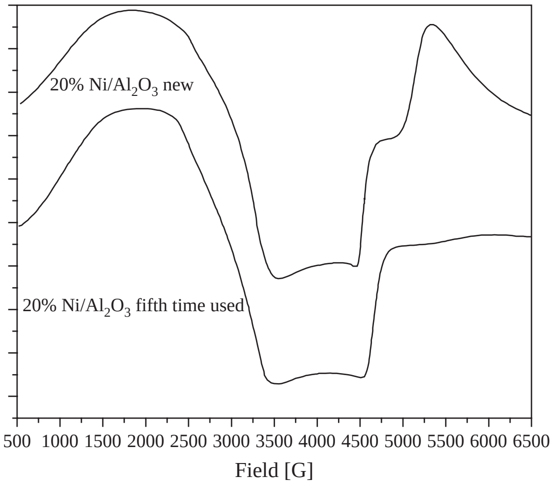

Figure 8. ESR spectra of 20 wt% Ni/Al$_2$O$_3$ catalyst, freshly prepared and after fifth time of using at 1:5 wt:wt of Ni:PNP.

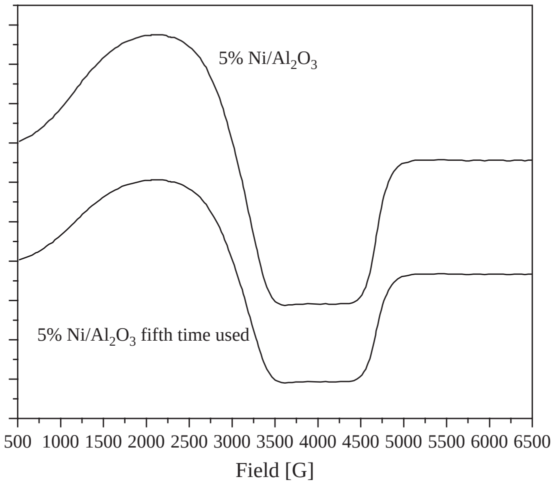

Figure 10. ESR spectra of 5 wt% Ni/Al$_2$O$_3$ catalyst, freshly prepared and after fifth time of using at 1:5 wt:wt of Ni:PNP.

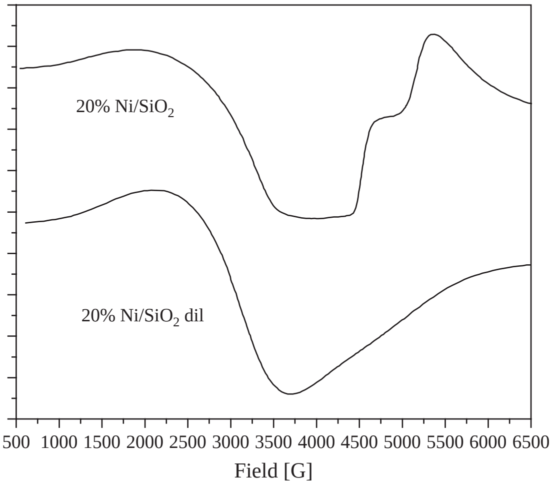

Figure 11. ESR spectra of 20 wt% Ni/SiO_2 as it is and after solid–solid dilution with bare SiO_2 till anisotropy disappears.

The same observation can be also shown in low loading samples of 5 wt% Ni (Figures 9 and 10).

In addition, the ESR spectra of commercial Raney nickel (Figure 12) showed a severe anisotropy, with low magnetic field overlapping signals. This behavior was also confirmed by similar catalytic activity of high loading catalyst and Raney nickel (Table 3).

Discussion

Hydrazine was utilized as the hydrogen donor in the reduction process of PNP over different nano supported nickel catalysts. The reaction was found to be completed within only a few minutes. In addition, the observable change in the color during the reaction from yellow to green to colorless, facilitated the suggestion of the mechanism of this reaction.

Table 1. Particle size of investigated samples using XRD and ESR.

	Particle size (nm)	
Catalyst	From XRD diffractograms	From ESR spectra
20 wt% Ni/SiO_2	40	15
20 wt% Ni/SiO_2 (fifth time used)	Amorphous	11
20 wt% Ni/Al_2O_3	36	16
20 wt% Ni/Al_2O_3 (fifth time used)	36	15
5 wt% Ni/SiO_2	40	19
5 wt% Ni/SiO_2 (second time used)	28.94	16
5 wt% Ni/Al_2O_3	34.30	14
5 wt% Ni/Al_2O_3 (fifth time used)	34.00	13
Commercial Raney nickel	–	15

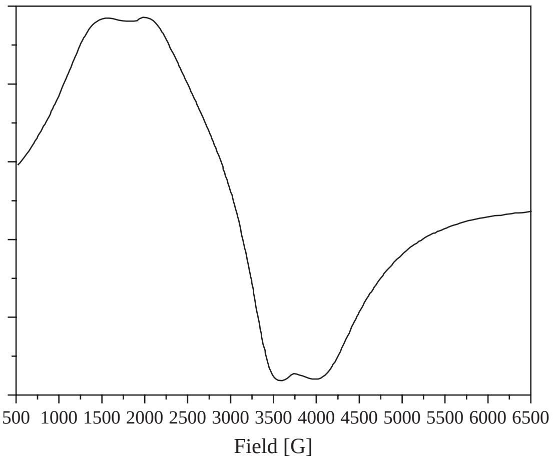

Figure 12. ESR spectra of commercial Raney nickel.

Mechanism of hydrogenation

During the hydrogenation process, the change in color was observed in a sequence of: (1) yellow color of PNP; (2) green color (intermediate A); and then (3) discharge of all color (PAP) accompanied with 100% conversion.

The following mechanism showed that H_2 (generated from the decomposition of hydrazine over Ni metal) is added first to the nitro group; after which, the elimination of two molecules of water was accompanied by a rearrangement of the molecule to form the green intermediate (A) (Scheme 1). The addition of another H_2 molecule to the green

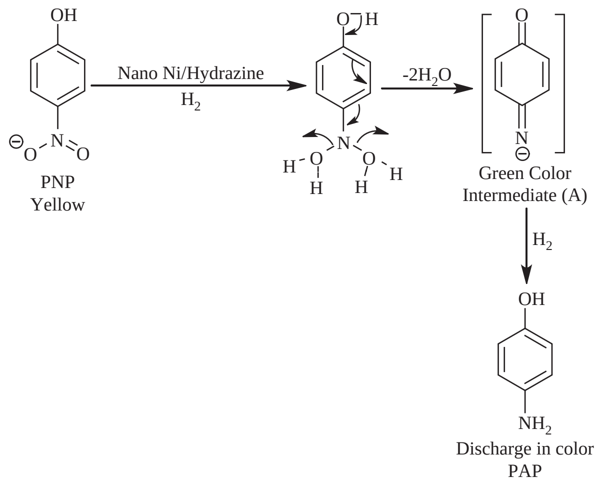

Scheme 1. Supposed mechanism for reduction process of *p*-nitrophenol.

intermediate is then accompanied by the formation of PAP.

Catalytic activity

Since the end of the reaction was found to be self indicated by a change in color at 100% conversion, the catalytic activity may be better expressed as the time to reach 100% conversion through this color change. Different ratios of PNP to Ni metal were varied and the catalytic activity of each was measured. Table 2 shows the time to completion for reactions with different concentrations of catalyst.

The results indicated that a 5 wt% Ni/Al_2O_3 is the best catalyst concentration, with the lower time to reach 100% conversion at different ratios of Ni:PNP.

Moreover, in order to completely characterize the catalyst we also studied the durability of the catalysts of 1:5 wt:wt Ni:PNP, using the catalyst up to five times as shown in Table 3.

Deeply analyzing the above data, very useful information regarding the catalytic activity of the catalysts prepared can be extracted. Thus, the catalytic activity of 5 wt% Ni supported on either SiO_2 or Al_2O_3 at lower ratios of Ni:PNP (1:5 wt:wt) exhibits a higher activity compared with those of higher loading of Ni (20 wt%). Moreover, at higher ratios of Ni:PNP (1:10 and 1:15 wt:wt) the 5 wt% Ni/Al_2O_3 showed superior catalytic activity compared to the 5 wt% Ni / SiO_2 support. This can be explained by the ease of transformation of crystalline nickel into amorphous phase over SiO_2 due to the weak metal support interaction. Moreover, the catalytic activity seems to be proportional to the crystalline nickel only. This behavior is confirmed during the durability test (Table 3) where a sharp decrease in the catalytic activity of 20 wt% Ni/SiO_2 at the fifth time of successive using (40 min) is accompanied with the disappearance of crystalline nickel, as shown by XRD diffractograms (Figure 1). In the same manner, the 5 wt% Ni/SiO_2 at the second time of use also showed the disappearance of crystalline nickel (Figure 3). Moreover, this behavior is accompanied by decrease in particle size of nickel as evidenced by ESR determination of particle size (Table 1).

Table 2. Effect of concentration of PNP:Ni on the catalytic activity.

Catalyst	wt:wt ratio of Ni:PNP 1:5	1:10	1:15	
20 wt% Ni/SiO_2	300	360	489	Time to reach 100% conversion (sec)
20 wt% Ni/Al_2O_3	300	390	420	
5 wt% Ni/SiO_2	300	420	527	
5 wt% Ni/Al_2O_3	80	190	200	

In addition, the increase of the catalytic activity of low loading Ni on both SiO_2 and Al_2O_3 supports suggests that not all nickel species act as active centers for this reaction. This can be viewed from two aspects, first, the increase of nickel loading will decrease the dispersion of nickel and hence not all nickel can be susceptible to the reactants; the second aspect is that the neighboring nano-sized nickel particles can influence each other as evidenced by ESR. It was also found that, as the amount of the existence of such strain among nano-nickel particles increases, the number of active nickel species decreases. Moreover, the catalytic activity was found to be proportional only to the crystalline nickel and this leads us to believe that the Al_2O_3 support is more effective than the SiO_2 support where, even at lower loading (5 wt%), the catalytic activity and durability are still very high.

In addition to all these observations, all catalyst samples were higher in catalytic activity than commercial Raney nickel. Moreover, the supported catalyst has the advantage of easily handling and the possibility of reuse of the catalyst more than one time, as compared to the impossibility to reuse Raney nickel where almost all nickel is lost during the filtration process at this low concentration of nickel.

Experimental

Materials

$NiSO_4.7H_2O$, $Al(OH)_3$, commercial Raney nickel, hydrazine hydrate 80%, PNP, PAP (as a standard materials), and methanol (spectroscopic grade) were purchased from Merck Co., Germany.

Commercial silica was obtained from Brownell limited Co., London. X-ray diffractograms were collected using Bruker D8 advance instrument with CuKα1 target operated at 40 kV and 40 mA. ESR spectra were measured using (Brucker Elexsys. 500) operated at X-band frequency. The following parameters are generalized to all samples otherwise mentioned in the text: microwave frequency, 9.73 GHz; receiver gain, 20; sweep width, 6000 center at 3480 G; and microwave power, 0.00202637 Watt.

Preparation

Nickel was loaded on Al_2O_3 (obtained by calcination of $Al(OH)_3$ at 550°C for 4 hours) and SiO_2 by means of impregnation method to be 20, 5, and 2.5 wt%. Hydrazine hydrate was used to reduce the catalysts in order to obtain the metallic form of nickel. Solid–solid

Table 3. Durability of the catalysts after five times of using at concentration of 1:5 wt:wt Ni:PNP.

	Number of successive uses of 1:5 wt:wt Ni:PNP					
Catalyst	1	2	3	4	5	
20 wt% Ni/SiO_2	240	240	383	1200	2400	Time to reach 100% conversion (sec)
20 wt% Ni/Al_2O_3	300	300	300	540	780	
5 wt% Ni/SiO_2	144	2100	–	–	–	
5 wt% Ni/Al_2O_3	80	93	100	240	240	
Commercial Raney nickel	260	–	–	–	–	

dilution is done by adding bare supports of SiO_2 or Al_2O_3.

Hydrogenation process

The hydrogenation process was performed by dissolving PNP in an appropriate amount of methanol followed by the addition of hydrazine hydrate as the hydrogen source and heating at 80°C. The catalyst was then added to the heated solution and the time to reach 100% conversion (as examined by thin layer chromatography (TLC) and IR spectra) was taken as an expression of the catalytic activity.

The filtrate was then evaporated at reduced pressure and the residue was recrystallized from hot water to give pure product of PAP in almost 100% yield.

The characteristics of the product, PAP, are listed below:

$$\mathrm{IR}{:}(\nu_{\max}/\mathrm{cm}^{-1}){:}3423, 3340\ (\mathrm{NH_2}), 3190\ (\mathrm{OH}).$$

^{1}H NMR DMSO-d_6, Δ (ppm): 5.98 (s, 1H, OH, D_2O – exchangeable), 6.42 (d, 2H, $J = 6.7$ Hz, ArH's), 6.99 (d, 2H, $J = 6.7$ Hz, ArH's), and 9.86 (br s, 2H, NH_2, D_2O – exchangeable).

Conclusion

In this study we found that the use of hydrazine as a hydrogen source was very effective for the reduction of PNP into PAP. The use of supported nano-sized nickel was found to be very effective in such reactions. The catalytic activity reached three times higher than the commercial Raney nickel in the case of 5 wt% Ni/Al_2O_3 catalyst. Of a much higher concern may be the possibility of reuse the supported catalysts more than one time in the reaction. The catalytic activity of nickel is influenced by the existence of strain among nano nickel particles and is proportional to only the crystalline nickel. Ni/Al_2O_3 catalyst has proved to be more effective than Ni/SiO_2 catalyst, where high durability and high catalytic activity of Ni/Al_2O_3 catalyst were attained. The mechanism of the hydrogenation reaction is guided according to the change in color during the reaction. The change in color in the reaction makes it a self-indicator of 100% conversion, which decreases the time and effort for following up the reaction.

References

(1) Trost, B.M. *Science* **1991,** *254,* 1471–1477.
(2) Sheldon, R.A. *Green Chem.* **2007,** *9*, 1273–1283.
(3) Rode, C.V.; Vaidya, M.J.; Jaganathan, R.; Chaudhari, R.V. *Chem. Eng. Sci.* **2001,** *56*, 1299–1304.
(4) Rode, C.V.; Vaidya, M.J.; Chaudhari, R.V. *Org. Process Res. Dev.* **1999,** *3*, 465–470.
(5) Komatsu, T.; Hirose, T. *Appl. Catal. A: Gen.* **2004,** *276*, 95–102.
(6) Sathe, S.S. Process for preparing *p*-aminophenol in the presence of dimethyldodecylamine sulfate. US Patent 4176138, 1979.
(7) Lee, L.T.; Chen, M.H.; Yao, C.N. Process for manufacturing *p*-aminophenol. US Patent 4885389, 1989.
(8) Yun, K.S.; Cho, B.W. Process for preparing para-aminophenol. US Patent 066369, 1991.
(9) Vaidya, M.J.; Kulkami, S.M.; Chaudhari, R.V. *Org. Process Res. Dev.* **2003,** *7*, 202–208.
(10) Venkatraman, K. *The Chemistry of Synthetic Dyes*; Academic Press: New York, 1952; Vol. I; p 184.
(11) House, H.O. *Modern Synthetic Reactions*, 2nd ed.; Benjamin: New York, 1977; p 145.
(12) Rylander, P.N. *Hydrogenation Methods*; Academic: New York, 1985; p 365.
(13) Popp, F.D.; Schultz, H.P. *Chem. Rev.* **1962,** *62*, 19.
(14) Harmon, R.E.; Gupta, S.K.; Brown, D.J. *Chem. Rev.* **1972,** *72*, 21–52.
(15) Chen, R.Z.; Du, Y.; Chen, C.L.; Xing, W.H.; Xu, N.P.; Chen, C.X.; Zhang, Z.L. *J. Chem. Ind. Eng. (China)* **2003,** *54*, 704–706.
(16) Du, Y.; Chen, H.L.; Chen, R.Z.; Xu, N.P. Synthesis of *p*-aminophenol from *p*-nitrophenol over nano-sized nickel catalysts. *Appl. Catal. A: Gen.* **2004,** *277*, 259–264.
(17) Rautanen, P.A.; Aittamaa, J.R.; Krause, A.O.I. *Chem. Eng. Sci.* **2001,** *56*, 1247–1253.
(18) Suh, D.J.; Park, T.J.; Lee, S.H.; Kim, K.L. *J. Non-Cryst. Solids* **2001,** *285*, 309–316.
(19) Wu, W.H.; Xu, J. *Catal. Commun.* **2004,** *5*, 591–595.

(20) Wu, W.H.; Xu, J.; Ohnishi, R. *Appl. Catal. B: Environ.* **2005,** *60*, 129–137.

(21) Kapoor, M.P.; Matsumura, Y. *J. Mol. Catal. A: Chem.* **2002,** *178*, 169–172.

(22) Toppinen, S.; Rantakyh, T.K.; Salmi, T.; Aittamaa, J. *Catal. Today* **1997,** *38*, 23–30.

(23) Quincoces, C.E.; Gonzfilez, M.G. Kinetic study on Coz refroming of methane. *Chin. J. Chem. Eng.* **2001,** *9*, 190–195.

(24) Rizhi, C.; Yan, D.U.; Weihong, X.; Nanping, X.U. *Chinese J. Chem. Eng.* **2006,** *14*, 665–669.

(25) Shankare, G.; Channe, G. *Tetrahedron* **2002,** *58*, 2211–2213.

(26) Chang, Y.C.; Chen, D.H. *J. Hazard Mater.* **2009**, *165*, 664–669.

(27) Yan, D.; Hongling, C.; Rizhi, C.; Nanping, X. *Appl Catal A: Gen.* **2004,** *277*, 259–264.

(28) Zhang, F.; Chan, S.W.; Spanier, J.E.; Apak, E.; Jin, Q.; Robinson, R.D.; Herman, I.P. *Appl. Phys. Lett.* **2002,** *80*, 127–129.

(29) Sharma, V.K.; Baiker, A. *J. Chem. Phys.* **1981,** *75*, 5596–5601.

(30) Suran, G.; Stankoff, A.; Hofmann, F. *Phys. Rev. B.* **1973,** *8*, 1109–1118.

(31) Kawabata, A. *J. Phys. Soc. Jpn.* **1970,** *29*, 902–911.

(32) Selim, M.M.; Abd El-Maksoud, I.H. *Microporous Mesoporous Mater.* **2005,** *85*, 273–278.